ACADEMIC PRESS

Available online at www.sciencedirect.com

SCIENCE DIRECT®

VIROLOGY

Virology 311 (2003) 275–288

www.elsevier.com/locate/yviro

Structural characterization of respiratory syncytial virus fusion inhibitor escape mutants: homology model of the F protein and a syncytium formation assay

Craig J. Morton,[a,*] Rachel Cameron,[a] Lynne J. Lawrence,[b,1] Bo Lin,[a] Melinda Lowe,[b] Angela Luttick,[a] Anthony Mason,[a] Jenny McKimm-Breschkin,[b,1] Michael W. Parker,[c] Jane Ryan,[a] Michael Smout,[d] Jayne Sullivan,[a] Simon P. Tucker,[a] and Paul R. Young[d]

[a] *Biota Holdings Limited, 616 St Kilda Road, Melbourne, Victoria 3004, Australia*
[b] *Biomolecular Research Institute, Parkville, Victoria 3052, Australia*
[c] *Biota Structural Biology Laboratory, St. Vincent's Institute of Medical Research, Fitzroy, Victoria 3065, Australia*
[d] *Department of Microbiology & Parasitology, School of Molecular and Microbial Sciences, University of Queensland, St. Lucia, Queensland 4072, Australia*

Received 3 July 2002; returned to author for revision 19 August 2002; accepted 20 December 2002

Abstract

Respiratory syncytial virus (RSV) is a ubiquitous human pathogen and the leading cause of lower respiratory tract infections in infants. Infection of cells and subsequent formation of syncytia occur through membrane fusion mediated by the RSV fusion protein (RSV-F). A novel *in vitro* assay of recombinant RSV-F function has been devised and used to characterize a number of escape mutants for three known inhibitors of RSV-F that have been isolated. Homology modeling of the RSV-F structure has been carried out on the basis of a chimera derived from the crystal structures of the RSV-F core and a fragment from the orthologous fusion protein from Newcastle disease virus (NDV). The structure correlates well with the appearance of RSV-F in electron micrographs, and the residues identified as contributing to specific binding sites for several monoclonal antibodies are arranged in appropriate solvent-accessible clusters. The positions of the characterized resistance mutants in the model structure identify two promising regions for the design of fusion inhibitors.

Keywords: Respiratory syncytial virus; Assay; Fusion protein; Homology model; Antiviral; Inhibitor

Introduction

Respiratory syncytial virus (RSV) is the predominant cause of acute lower respiratory tract infection in children, with symptoms ranging from severe pneumonia and bronchiolitis to much milder infections similar to the common cold (Cane, 2001, Collins et al., 1996). While primary infection does generate a long-term immune response this is not fully protective and recurrent infection can occur throughout life, with annual reinfection rates of 3–6% in adults (Monto and Lim, 1971). RSV infection is also a major cause of morbidity and mortality in institutionalized elderly and immunocompromised adults (Collins et al., 1996).

RSV is a member of the *Pneumovirus* genus of the family *Paramyxoviridae*, which includes other human pathogens such as mumps, measles, and the parainfluenza viruses. The RSV genome is a single strand of negative-sense RNA encoding 10 proteins. Three viral proteins, G, F, and SH, are located on the surface of infected cells and virions. While G and SH are believed to play a significant role in attachment and entry, the F glycoprotein is necessary and sufficient for viral infection and the fusion of infected cells with their neighbors to form syncytia (Kahn et al., 1999; Techaarpornkul et al., 2001).

* Corresponding author. Biota Structural Biology Laboratory, St. Vincent's Institute of Medical Research, 9 Princes Street, Fitzroy, Victoria 3065, Australia. Fax: +61-3-9416-2676.

E-mail address: craig@medstv.unimelb.edu.au (C.J. Morton).

[1] Present address: CSIRO Health Sciences and Nutrition, Parkville, Victoria 3052, Australia (L.J. Lawrence, J. McKimm-Breschkin).

0042-6822/03/$ – see front matter © 2003 Elsevier Science (USA). All rights reserved.
doi:10.1016/S0042-6822(03)00115-6

RSV-F is expressed as a single precursor of 574 amino acids, F_0, which oligomerizes in the endoplasmic reticulum and is proteolytically processed at two sites in each monomer, resulting in an oligomer of two disulfide-linked fragments: F_2 (the smaller N-terminal fragment) and F_1. The protein is anchored in membranes through a hydrophobic peptide in the C-terminal region of F_1 which is followed by a 24-amino-acid cytoplasmic tail. The protein is also glycosylated at five or six potential N-linked sites located principally in F_2 and contains palmitate (Collins et al., 1996). RSV-F is believed to adopt a metastable prefusogenic conformation until triggered in the presence of a target membrane and/or receptor. Triggering of the protein is thought to result in a conformational change that exposes a very hydrophobic stretch of residues at the extreme N terminus of F_1, known as the fusion peptide. It is generally believed that the fusion peptide associates with the target cell membrane on exposure. In this model, the change from the prefusogenic structure to the final fusogenic conformation of the protein brings the fusion peptide into close proximity to the anchor sequence, promoting the fusion of the virus (and/or infected cell) membrane with the target cell membrane.

The structure of a fragment of the fusion protein of Newcastle disease virus (NDV) has been reported at a resolution of 3.3 Å (Chen et al., 2001). This protein has some similarity in both sequence and mode of action to the RSV fusion protein. Only 355 of the 553 residues in the NDV fusion protein were present in the final crystal form (residues 33–105 and 171–454), such that important regions of the protein structure were absent. Another structure was subsequently reported for the core fragment of RSV-F itself (Zhao et al., 2000) which included a large section of the protein absent from the NDV-F structure.

We report herein a novel syncytium formation assay for activity of recombinant RSV-F expressed from an optimized gene construct that allows rapid in vitro assessment of fusion inhibitors and the analysis of resistance mutations. We also describe the structure of the majority of the RSV-F protein produced by molecular modeling on the basis of a chimera devised by combining the fragmentary NDV-F crystal structure with the structure of the RSV-F core. We have employed this model as a tool to reach a greater understanding of the mechanism of action of RSV-F inhibitors and the nature of known sites of neutralizing antibody binding.

Results and discussion

Syncytium formation assay using recombinant RSV-F in mammalian cells

Initial attempts to express RSV-F using viral cDNA fragments derived from RT-PCR of viral mRNA were unsuccessful. Constructs designed to express either the full-length version of F or a soluble version of F lacking the transmembrane and cytoplasmic regions failed to elicit significant expression when tested in transient assays in 293 cells. Reasons for low expression could include: the high percentage of rare codons present in the RSV-F coding region, the presence of multiple poly-(A) addition sequences, and the presence of splice acceptor and donor sites within the coding region. A synthetic RSV-F construct was therefore assembled incorporating optimized codon usage and with potential poly-(A) and splice sites removed (Mason et al., 2000). The construct also incorporated multiple unique restriction sites to simplify subsequent mutagenesis studies.

Analysis of expression of both the soluble and transmembrane synthetic F constructs showed that RSV-F expression levels improved by at least 20- to 50-fold compared with RSV-F natural sequence vectors (data not shown). Although recent reports have indicated that RSV-F is sufficient to support viral entry (Techaarpornkul et al., 2001) and induce syncytium formation in a vesicular stomatitis virus background (Kahn et al., 1999), previous reports have shown that RSV-F, -G, and -SH are required for efficient fusion when vaccinia virus vectors are used (Heminway et al., 1994). The possible contribution of other viral proteins derived from RSV or the viral expression systems to F function in these systems has not been elucidated. Extensive syncytium formation was observed 48 h post-transfection of just the synthetic F construct into 293 cells (Fig. 1A), indicating that F alone is sufficient for membrane fusion. In contrast, 293 cells transfected under identical conditions with an equivalent plasmid expressing RSV A2 F natural codon sequence (Fig. 1B) appeared similar to the mock-transfected control (Fig. 1C). In addition, we observed that the size and extent of syncytium formation in 293 cells expressing F from the synthetic gene were unaffected by coexpression of codon-optimized constructs for RSV-G or RSV-SH, neither of which initiate syncytium formation when expressed alone (Heminway et al., 1994) and that known fusion inhibitors prevented syncytium formation in a concentration-dependent manner (Fig. 2, Table 1). To our knowledge, this is the first demonstration of cellular fusion mediated by RSV-F in the absence of any other viral proteins, and provides an assay system for analysis of RSV-F inhibitors and mutants that is free of the confounding variables that may potentially be introduced by coexpression of other viral gene products.

Identification of RSV-F escape mutants

A combination of serial passage and the syncytium formation assay was used to identify RSV-F inhibitor escape mutants. Three published RSV-F inhibitors were used to raise inhibitor-resistance mutant viruses. Escape mutants for each compound (Fig. 3: compound 1: VP14637 Viropharma Inc., Patent WO 99/38508; compound 2: R170591, Jannsen Pharmaceutica, Patent WO 01/00612; compound 3: CL-

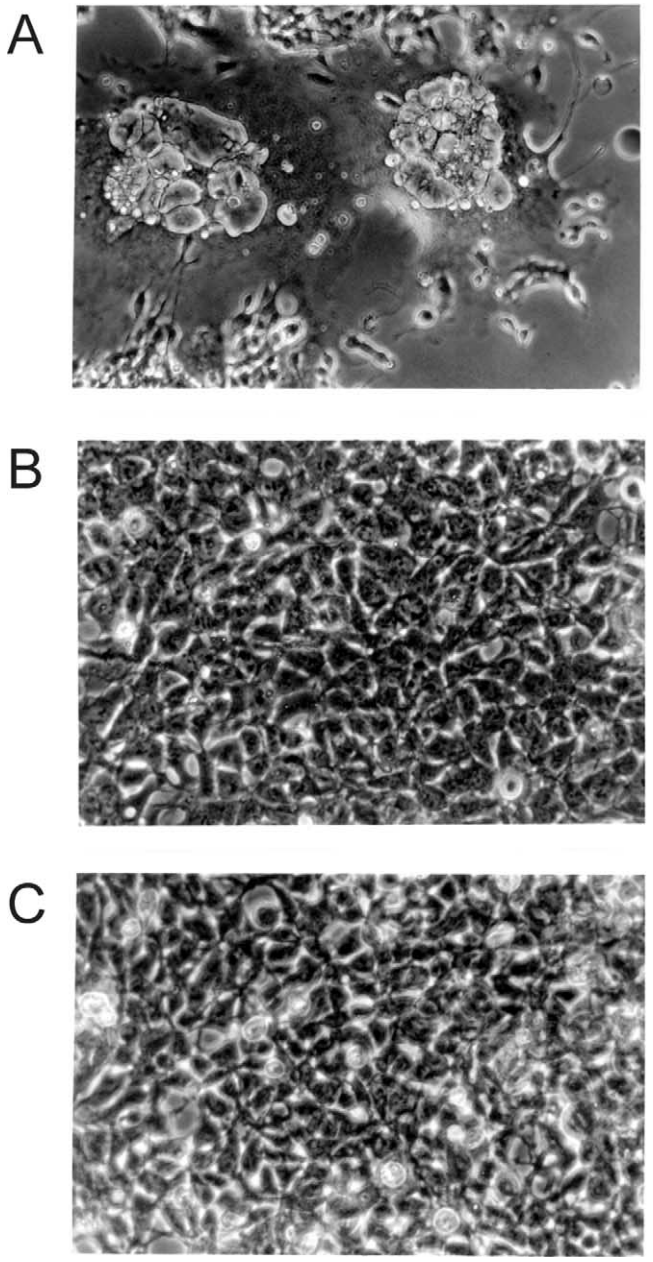

Fig. 1. Formation of syncytia in cell cultures transfected with expression plasmids for RSV-F constructs. Transfection with plasmid expressing the codon-optimized RSV-F construct pCICO.F.FL.opt (A) causes substantially greater levels of syncytium formation compared with transfection with wild-type RSV-F (B). Mock-transfected cells show no syncytium formation and remain confluent (C). In all cases photographs were taken of cells 48 h posttransfection at 400× magnification.

387626, Wyeth–Ayerst Research (Wyde et al., 1998)) were isolated by serial passage of the virus in the presence of the inhibitor (Table 2). The F genes of resistant viruses were sequenced and the sites of mutation identified.

A total of nine distinct escape mutations across eight different resistant isolates were characterized for the three compounds tested (Table 2). Two distinct sets of mutation hotspots were identified: one corresponding to resistance to compounds 1 and 2, the other to escape from inhibition by compound 3. As these data show, compounds 1 and 2, while structurally dissimilar, gave rise to very similar resistance mutations and showed cross-sensitivity, in that mutations identified as giving resistance to compound 1 also gave rise to equivalent resistance to compound 2 and vice versa. All mutations identified in the resistant isolates were analysed in the syncytium formation assay to confirm that they were responsible for the observed inhibitor resistance (Table 1). A selection of the scoring data for one of the resistance mutants is shown graphically in Fig. 4 to highlight the clarity of results from the assay.

Recombinant F protein expression and electron microscopy

While providing adequate expression levels of RSV-F for assay purposes, the yield of protein in the mammalian expression system was too low for any detailed structural studies. To generate high levels of the F glycoprotein for analysis, we constructed a recombinant baculovirus that expressed a secreted form of F in which the transmembrane and cytoplasmic tail domains were replaced by a C-terminal six-histidine tag. The recombinant RSV-F was purified from infected culture medium harvests by Ni^{2+}- affinity chromatography and analyzed by SDS-PAGE (Fig. 5A). Overexpression of the wild-type RSV A2 F sequence in this system always yielded two species migrating with molecular weights of approximately 72 and 62 kDa (**1** and **2** respectively in Fig. 5A). Analysis under reducing conditions revealed that these species comprised disulfide-bonded fragments and a variable amount (depending on the preparation) of uncleaved F_0. N-terminal sequencing of the resulting 50- and 46-kDa fragments (Fig. 5A, F_1+ and F_1, respectively) revealed that cleavage of the F_0 precursor had occurred at two independent sites. Site 1 cleavage (^{133}RKRR/FLGF^{140}) generated the expected F_1 fragment reported for RSV F (46 kDa) but a second cleavage site (^{106}RARR/ELPR^{113}), N terminal to a stretch of amino acids unique to RSV-F, generated the additional fragment F_1+. We subsequently confirmed that this second cleavage site was essential for fusion activation (Mason et al., 2000) as has subsequently been shown by others (Gonzalez-Reyes et al., 2001; Zimmer et al., 2001). Endoglycosidase digestions further showed that the F_2 fragments of 19 and 16 kDa were glycosylation variants, most likely comprising carbohydrate moieties at two and one of the available sites, respectively. A schematic summary of these findings is presented in Fig. 5B.

Recombinant RSV-F purified from baculovirus vector-infected culture supernatants was examined by electron microscopy to determine gross characteristics of protein structure (Fig. 5C). In agreement with work reported by others (Calder et al., 2000; Gonzalez-Reyes et al., 2001), two different RSV-F conformations were observed, previously described as “cones” and “lollipops,” which may correspond to prefusogenic and fusogenic structures of the pro-

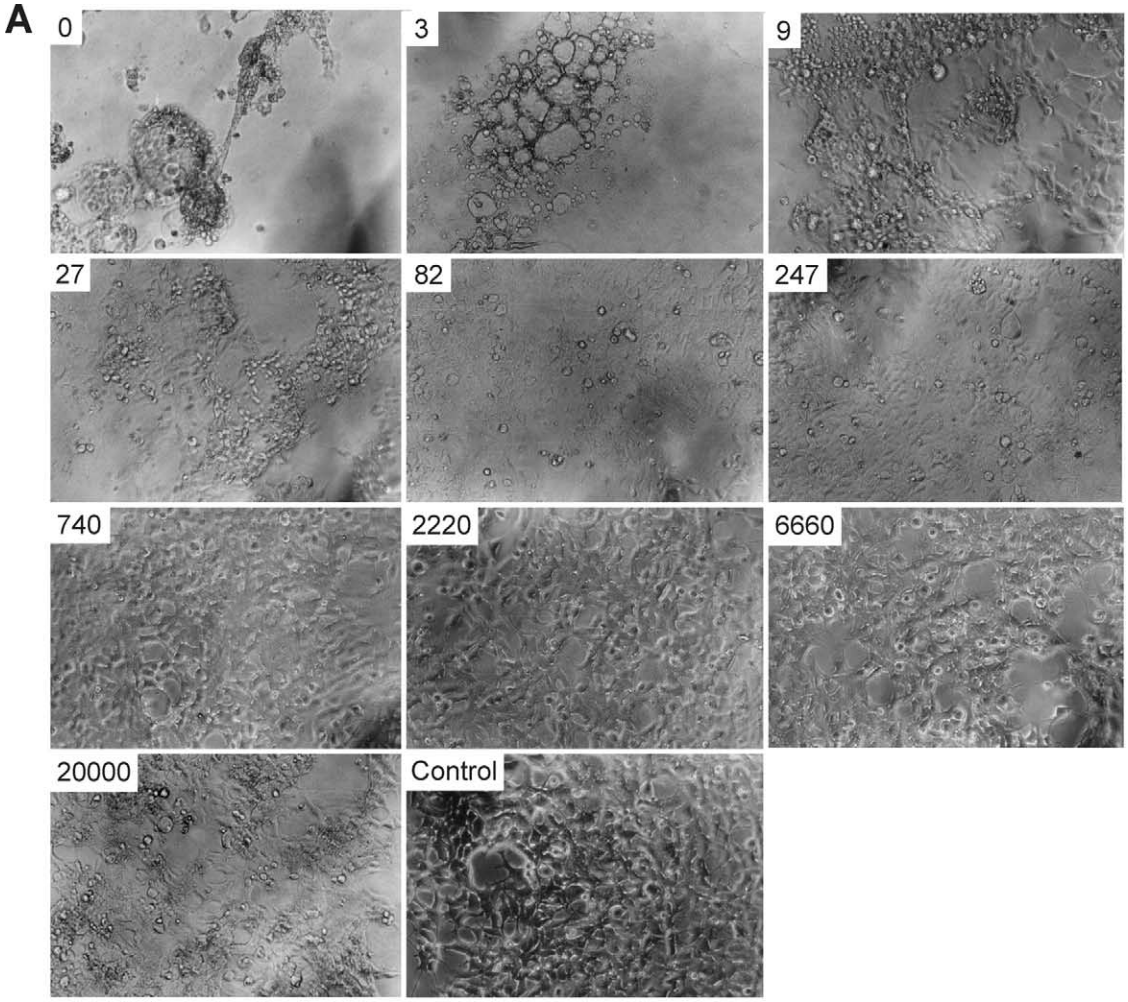
A
0
3
9
27
82
247
740
2220
6660
20000
Control

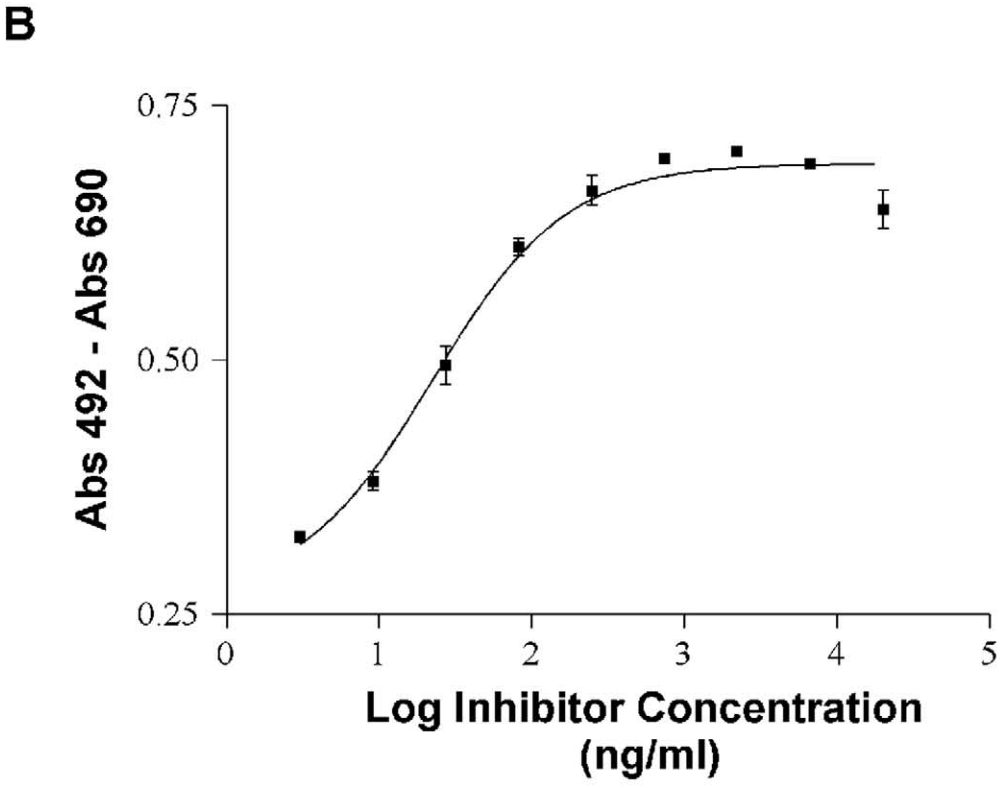
B
0.75
0.50
0.25
Abs 492 - Abs 690
0
1
2
3
4
5
Log Inhibitor Concentration
(ng/ml)

Table 1
Syncytium formation assay results for a selection of inhibitor resistance mutants[a]

RSV-F construct	EC_{50} (ng/ml)		
	Compound 1	Compound 2	Compound 3
Wild type	24	97	2100
F488L	NI	NI	7600
D486N	NI	nt[b]	4300
V76A, G446E, N517I	3	8	NI
N517I	18	125	4100
V76A	29	97	3000
G446E	2	9	NI

[a] Constructs containing the listed mutations were transfected into 292 cells and the level of syncytium formation in the presence of serial dilutions of each inhibitor was determined. EC_{50} values for each mutant were calculated from computational fitting of the data to a sigmoidal dose–response curve. A value of NI indicates no inhibition seen at the highest concentration of inhibitor tested. The three compounds are (1) VP14637 (Patent WO 99/38508), (2) R170591 (Patent WO 01/00612), and (3) CL-387626 (Wyde et al., 1998).

[b] nt, not tested.

tein. Both single trimeric species (mostly "cones") and rosettes (comprising mostly "lollipops") can be seen in these preparations. This is the first demonstration of high-level expression of recombinant RSV-F and demonstrates that the overall morphology and processing of the recombinant protein are the same as found in native expression.

Molecular modeling

The model structure for the postfusion conformation of residues 29 to 98 and 160 to 515 of RSV-F is shown in Fig. 6 with details of the alignment between the RSV-F and NDV-F sequences and secondary structure predictions used to build the model. The excellent agreement between the predicted secondary structure for RSV-F and NDV-F and the experimental secondary structure derived from the NDV-F crystal increases confidence in the accuracy of the model despite the rather low level of sequence identity between the two proteins. The RSV-F protein consists of a trimer of disulfide-linked F_2–F_1 pairs arranged with three-fold symmetry about a central axis. As described in the published work detailing the structure of the related viral fusion protein NDV-F (Chen et al., 2001), the protein can be divided on inspection into three regions. The base is an elongated stalk, consisting primarily of a six-membered antiparallel helical coiled-coil (the "core" region of the protein (Zhao et al., 2000)) composed of the two heptad-repeat regions, HR-1 and HR-2, previously identified in the RSV-F sequence (Chambers et al., 1990) and shown to adopt a six-membered trimeric coiled coil in solution (Lawless-Delmedico et al., 2000; Matthews et al., 2000).

The head region, approximately the shape of an inverted triangular prism, has a large central cavity accessible to the exterior of the protein through a channel down the axis of the protein and three symmetrically positioned radial channels. Between these two sections of the protein is an interface described as the neck region. The approximate dimensions of the protein measured from the electron micrographs (25 to 30 nm in length, Fig. 5C) are in good agreement with the size of the protein in the homology model. Note in particular that for most of the structures an electron-dense center can be seen in the head of the spike that may correspond to the radial channels observed in the model.

As Chen and colleagues noted for NDV-F (see Fig. 7 in Chen et al., 2001), the structure has obvious implications for a possible mode of action of RSV-F, wherein the fusion peptides at the end of HR-1 are sequestered in some undefined manner within the head of the protein, only to be released when contact with a target cell triggers the exposure of the fusion peptides which then bury within the target cell membrane. A rearrangement of the conformation of the F protein then brings the fusion peptides and viral anchor peptides into close proximity (as in the fusion-activated homology model presented in Fig. 6), simultaneously resulting in the fusion of the two membranes. In the EM images, aggregation of trimeric units into rosettes always involved interactions at the base of the stalk. The RSV-F protein model suggests that this is likely to be a consequence of hydrophobic interactions between the fusion domains at the base of the stalk following conformational reorganization.

Correct identification of the model as representing the postfusion form of RSV-F is essential if the structure is to be correctly interpreted. The NDV-F crystal structure was determined using crystals grown from inactivated F_0 protein (Chen et al., 2001) but the authors are noncommittal on whether the structure is of F_0 or some other form of the protein that has undergone proteolytic activation. Two observations in particular suggest that the structure is of postfusion protein. First, the NDV-F structure on which it is based showed well-defined central and radial channels in which one would expect the fusion peptide to be buried in the prefusion structure of the protein. The absence of electron density in these channels, which correspond to the

Fig. 2. Effect of an RSV-F inhibitor on fusion activity in the syncytium formation assay. Cells were transfected with plasmid expressing a codon-optimized RSV-F construct in the presence of increasing concentrations of VP14637, a known inhibitor of RSV-F activity. (A) Photographs of cells taken 48 h posttransfection at 400× magnification. Concentration of inhibitor (in ng/ml) is indicated in each photograph. Control cells were transfected with plasmid lacking the RSV-F construct. In the absence of inhibitor cell death due to syncytium formation is complete, while at high concentrations a degree of inhibitor-induced cell death occurs. (B) Graph of quantitated syncytium formation at different inhibitor concentrations. Each data point corresponds to one of the photographs in (A), allowing correlation of the degree of syncytium formation with the experimental score. The drop in absorbance values at high concentrations of inhibitor correlates with the cell death seen in the photographs.

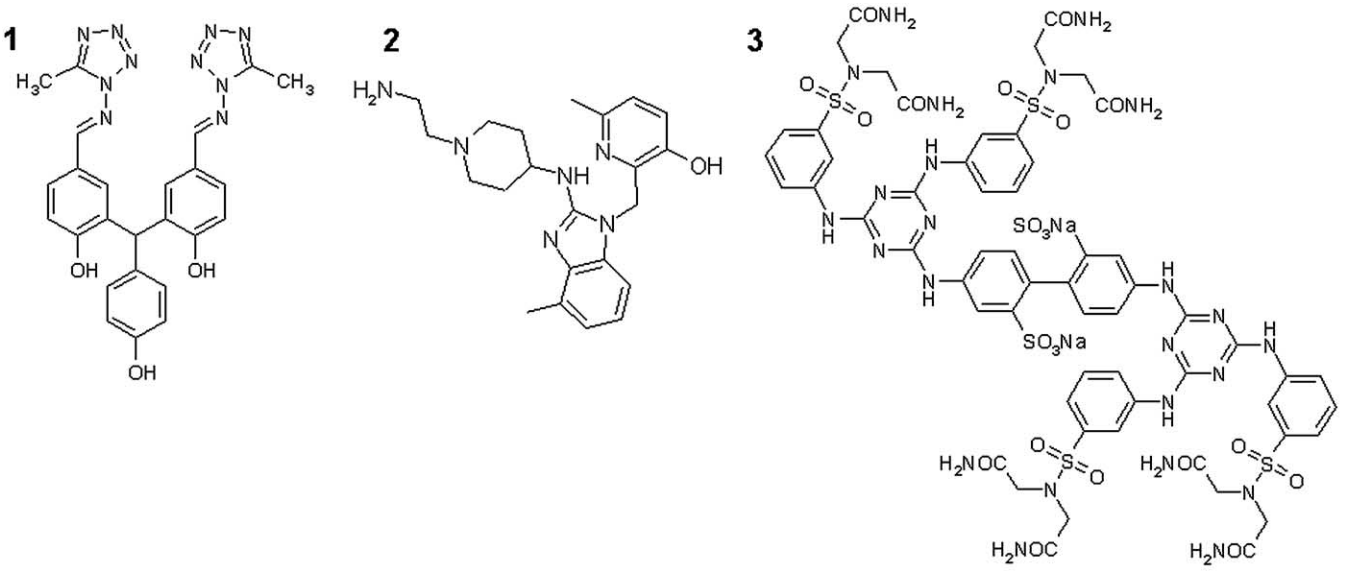

Fig. 3. Structures of three known RSV-F inhibitors: (1) VP14637 (Patent WO 99/38508), (2) R170591 (Patent WO 01/00612), (3) CL-387626 (Wyde et al., 1998).

cavities seen in EM images of postfusion RSV-F (Fig. 5C), suggests that the fusion peptides have been revealed and are no longer sequestered within the head. Second, the surprisingly good correlation between the position of the ends of the NDV-F structure and those of the RSV core structure implies that the NDV-F protein had formed an equivalent coiled-coil core region, characteristic of the postfusion form of the protein. Other lines of evidence, such as the burial of a known antigenic region of the protein and putative modes of action for two fusion inhibitors (see below), support the identification of the structure of the RSV-F model and the NDV-F crystal structure as the postfusion form of the proteins.

A model of the RSV-F protein based on the NDV-F crystal structure has previously been published by Smith and colleagues (2002). This model is based solely on the NDV-F structure and thus lacks the majority of the helical coiled coil that constitutes the stalk region of the protein. Combination of the RSV core and NDV-F structures circumvents this problem and allows a clearer view of the entire RSV-F structure. Comparison of the sequence alignments used here (Fig. 6B) and by Smith et al. show few differences and visual inspection of the two models suggests that the overall structures of those regions common to both models are very similar.

Table 2
EC_{50} of resistance mutants to three RSV fusion inhibitors identified from virus culture in the presence of the inhibitor[a]

Mutant isolated (virus strain)	Compound used for selection	Mean ± SD EC_{50} (ng/ml)		
		Compound 1	Compound 2	Compound 3
Wt (A2)[b]	None	0.4 ± 0.2 ($n = 6$)	0.8 ± 0.6 ($n = 6$)	414.1 ± 140.9 ($n = 6$)
Wt (Long)	None	0.6 ± 0.2 ($n = 6$)	3.0 ± 0.9 ($n = 6$)	186.2 ± 47.4 ($n = 6$)
Wt (B1)	None	1.4 ± 0.4 ($n = 6$)	9.9 ± 7.5 ($n = 6$)	80.0 ± 6.9 ($n = 6$)
F488I (A2)	1	>10,000	>10,000	1698.2
F488L, N517I (A2)	1	>10,000	>10,000	609.5
D489Y (Long)	1	>10,000	>10,000	260.7
D489Y (Long)	2	nt[c]	nt	nt
D486N (Long)	2	[d]	[d]	[d]
D486E (B1)	1	[d]	[d]	[d]
F488V (B1)	1	[d]	[d]	[d]
V76A, G446E, N517I (A2)	3	nt	nt	75,000 ± 5400 ($n = 2$)

[a] Viruses were cultured in the presence of compounds, the resistant strains isolated, and their F-protein genes sequenced. Cross-reactivity was tested by the CPE reduction assay in the presence of other compounds. The three compounds are (1) VP14637 (Patent WO 99/38508), (2) R170591 (Patent WO 01/00612), and (3) CL-387626 (Wyde et al., 1998).

[b] Wt, wild-type RSV A2, Long or B1. Variants are noted by reference to the amino acid substitution coded within the respective F genes.

[c] nt, not tested.

[d] Virus titer insufficient for CPE assay.

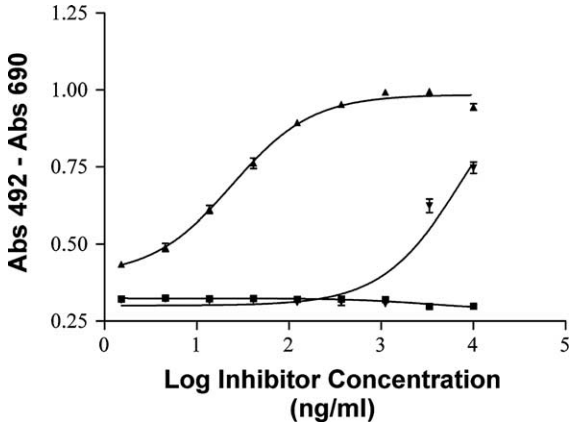

Fig. 4. Graph showing the syncytium formation assay results for an RSV-F construct carrying the mutation F488L. The three curves show the susceptibility of wild-type F to VP14637, a known inhibitor of RSV-F activity (▲, EC_{50} 24 ng/ml); the complete resistance to VP14637 seen for the construct carrying the mutation F488L (■, EC_{50} unmeasurable); and the continued susceptibility of the F488L mutant to CL-387626, a less active inhibitor of RSV-F that acts on a different site than does VP14637 (▼, EC_{50} 7.6 μg/ml). The curve shown for each data set was calculated by fitting to a sigmoidal dose–response model.

Characterization of sites of inhibitor escape mutants

The majority of the mutations identified as resulting in resistance to compounds 1 and 2 were found to cluster around F488 (Fig. 7), which fits into a hydrophobic pocket on the face of the internal helical bundle of the RSV-F core (Zhao et al., 2000). Equivalent pockets in the coiled-coil regions of other related fusion proteins, such as HIV gp41, are well characterized as sites of inhibitory action for both small molecule (Zhou et al., 2000) and peptidic (Eckert et al., 1999) inhibitors. Other mutations (e.g., N517I) present in the F gene of viruses exposed to compounds 1 and 2 were sometimes found in combination with those adjacent to the hydrophobic pocket, but in all cases these were shown to have no influence on inhibitor action when examined individually in the syncytium formation assay (Table 1).

A completely different site of mutation was identified for resistance to compound 3. Selection for resistance to compound 3 resulted in the isolation of a virus bearing three mutations in the RSV-F sequence: V76A, G446E, and N517I. Analysis of all eight possible combinations of these three mutations in the syncytium formation assay demonstrated that G446E was solely responsible for resistance to compound 3 although protein carrying this substitution was less efficient at inducing fusion in the absence of the other mutations (Table 1). G446 lies on the side of the head region, surrounded by a cluster of basic residues in our model (Fig. 7). The introduction of a negatively charged glutamate at this position may act to reduce the affinity of

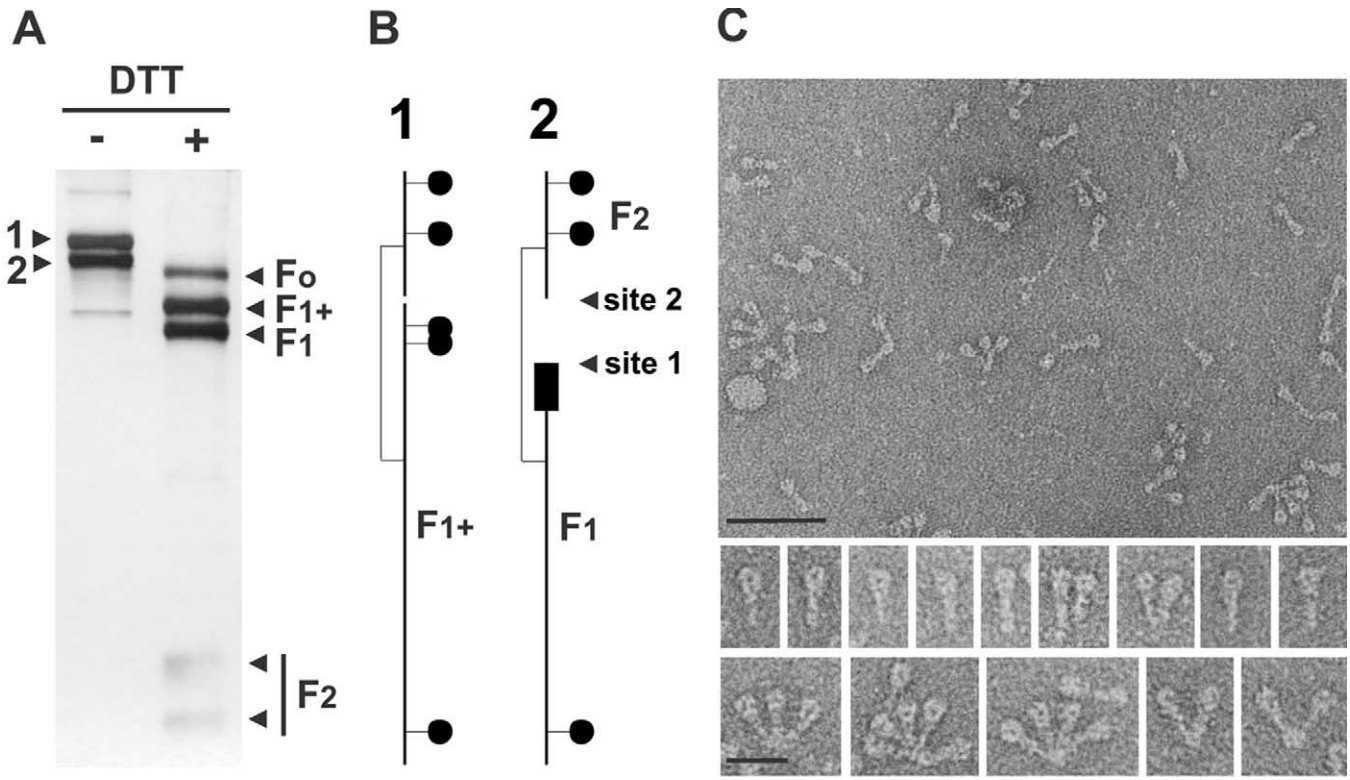

Fig. 5. Recombinant RSV-F protein. (A) Coomassie blue stained SDS–PAGE profile of nonreduced and reduced RSV-F purified from recombinant baculovirus-infected cultures. Uncleaved F_0 and cleaved fragments F_1, F_1+, and F_2 are indicated. (B) Schematic representation of the differentially cleaved RSV-F recombinant protein. The two independent cleavage sites are indicated: site 1 (^{133}RKRR/FLGF^{140}) and site 2 (^{106}RARR/ELPR^{113}). Potential sites of N-linked carbohydrate addition are indicated by attached circles, and numbers above the two schematics correspond to species identified in the gel profile shown in (A). (C) Electron micrographs of recombinant RSV-F expressed, secreted, and purified from baculovirus-infected insect cell cultures. Bars t 50 nm (top panel) and 20 nm (bottom panels).

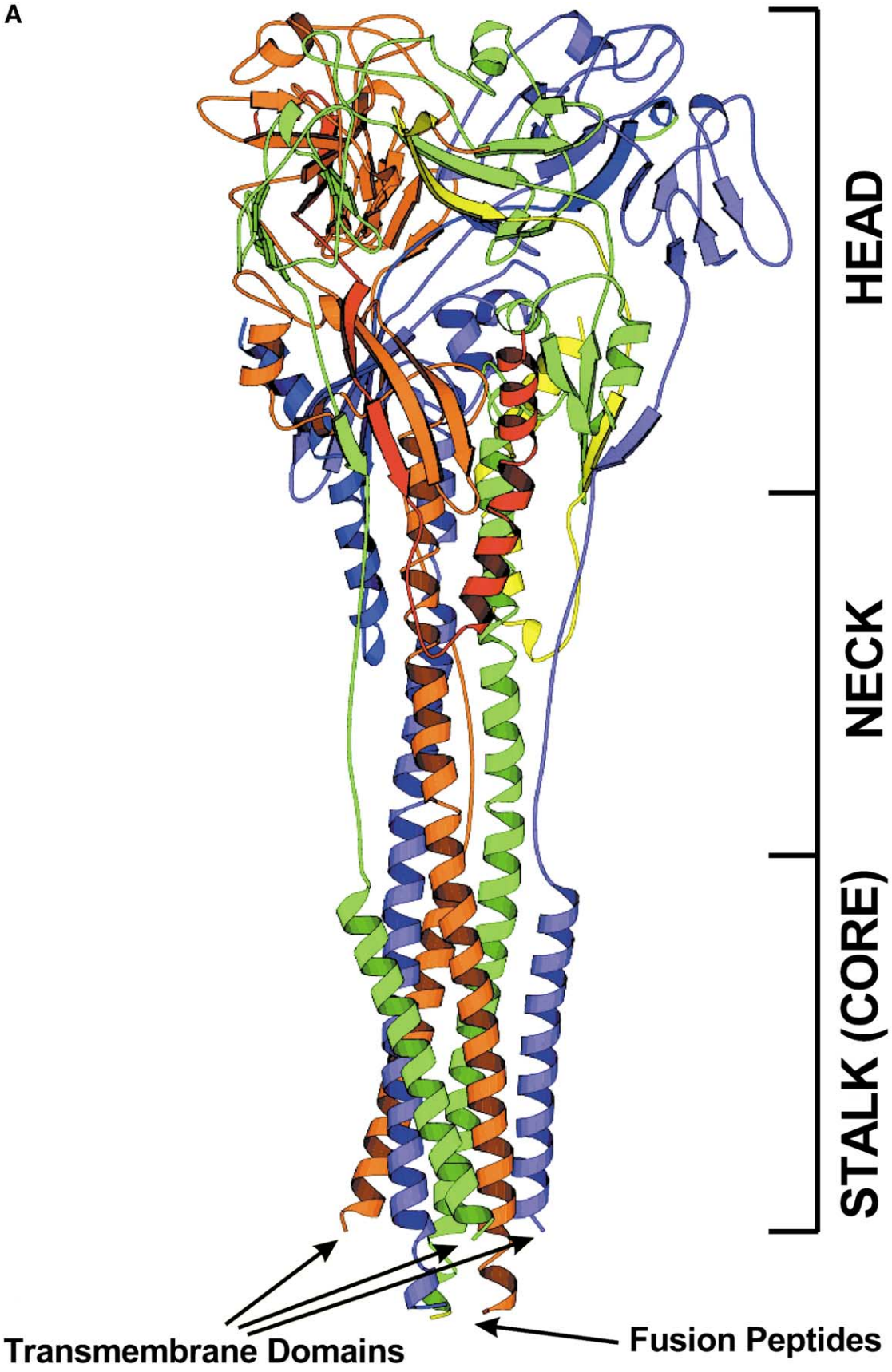
A
HEAD
NECK
STALK (CORE)
Transmembrane Domains
Fusion Peptides

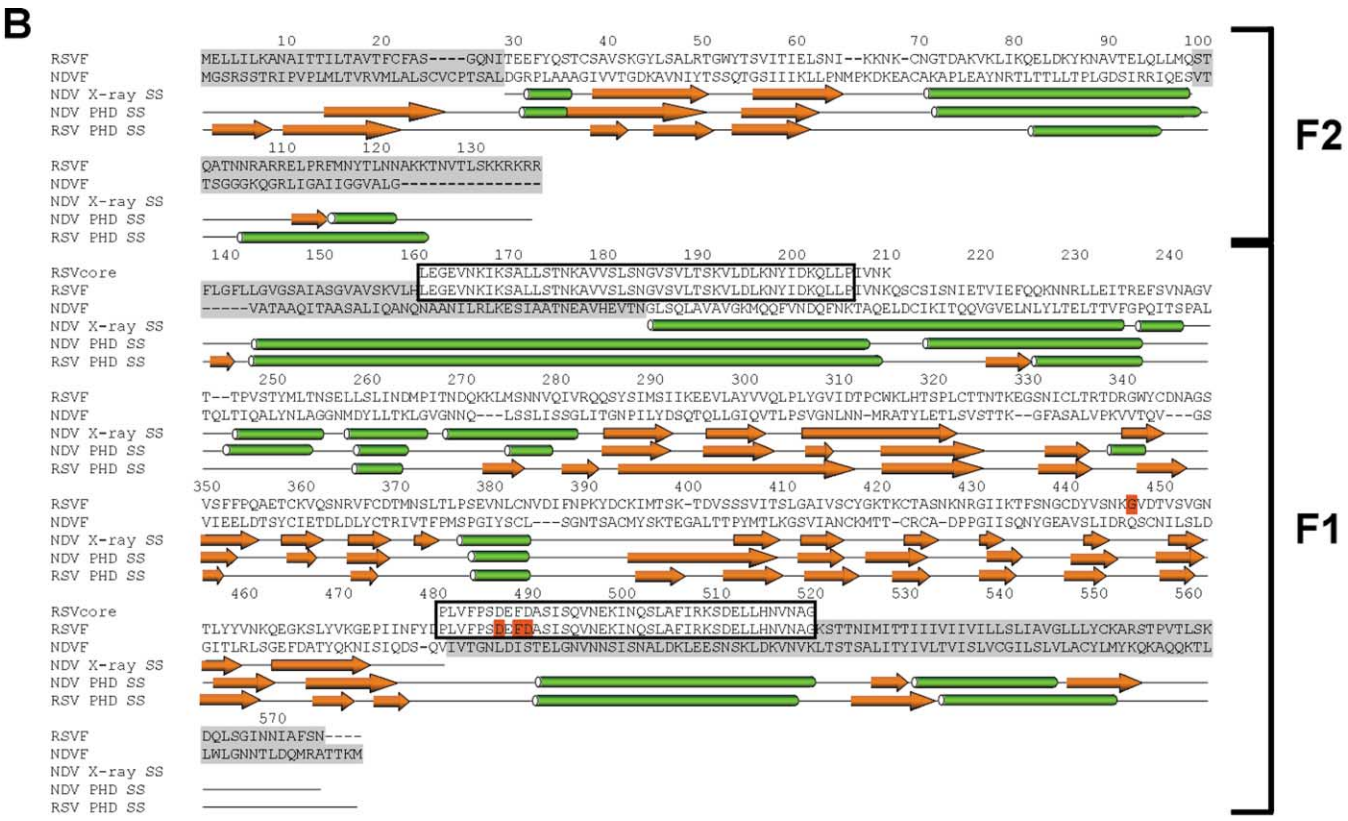

Fig. 6 (*continued*)

compound 3, which contains negatively charged sulfonic acid groups, with the basic residues surrounding the point of mutation. The role of this cluster of basic residues in the function of RSV-F is unclear, but there is strong evidence that RSV-F interacts with heparin or other glycosaminoglycans (GAGs) on the cell surface (Martinez and Melero, 2000; Hallak et al., 2000; Karger et al., 2000). It may be that this interaction is partly mediated by these basic residues and that compound 3 disrupts the binding to GAG. Interestingly, RSV-F constructs containing the G446E mutation appear to be slightly more susceptible to inhibition by compounds 1 and 2 than the wild-type protein (Table 1). This may be a consequence of the reduced levels of syncytium formation seen for G446E mutants even in the absence of inhibitor, possibly due to a reduced affinity for target cells.

Antibody binding sites

Antigenic sites on RSV-F have been found to cluster in immunogenic hotspots (Collins et al., 1996; Lopez et al., 1996) and the positions of some of these sites investigated by electron microscopy of RSV-F–antibody complexes (Calder et al., 2000). Several of these were mapped on the RSV-F model of Smith and colleagues (2002) and were shown to be in good agreement with the published EM data. As expected from the similarities between the model published here and that of Smith et al., (2002), the position of the antigenic sites derived from EM studies of antibody-bound RSV-F are also in good agreement with our model: site I (Fig. 8, green) located toward the top of the head, site II (Fig. 8, red) at the base of the neck, and sites IV, V, and VI (Fig. 8, blue) overlapping on the side of the head (see Fig. 4 in Calder et al., 2000). The residues forming site II have been predicted to form a helix–turn–helix structure (Lopez et al., 1996; Chambers et al., 1992) and were shown to do so as a 21-residue peptide in 30% trifluoroethanol (Toiron et al., 1996). This section of the protein forms a helix–turn–helix structure in our model that is fully exposed on the edge of one of the radial channels. If, as hypothesized, the radial channels play a critical role in the function

Fig. 6. (A) Diagrammatic representation of the structure of the homology model of RSV-F. The protein is colored by chain, with the F_1 subunits in orange, green, and violet and the F_2 subunits in red, yellow, and blue. The division of the structure into head, neck, and stalk (or core) regions is indicated, as are the attachment points for the three viral anchor peptides and three fusion peptides, which are not included in the model. (B) Sequence alignment of RSV-F, the RSV-F core, and NDV-F used for model building. Regions shaded gray in NDV-F were not present in the crystal structure. Regions of the RSV-F sequence that are shaded blue were modeled on the structure of the RSV-F core rather than on the structure of NDV-F, where it was present. Gray shading of the RSV-F sequence indicates regions that are absent from the modeled structure.

of the F protein as entry points for burial of the fusion peptide in the prefusogenic structure, then the potential impact of antibody binding immediately adjacent to the channel is clear. Sites IV, V, and VI are in very close proximity to the site of the resistance mutation for compound 3, G446E (Fig. 7), suggesting a possible similar mode of action for neutralizing antibodies that bind in this region.

A discrepancy is apparent between the model RSV-F structure and the predicted location of another immunogenic region comprising residues 205 to 237 (Fig. 8, orange and purple). These residues are almost totally concealed within the neck region of the RSV-F model, with only approximately 1000 $Å^2$ of a total potential surface of 6500 $Å^2$ exposed. Two overlapping peptides from this region react with neutralizing sera from RSV-infected animals and induce neutralizing antibodies to RSV (Collins et al., 1996). All of the surface exposed in the model originates in residues from the first peptide (residues 205–221, Fig. 8, orange), with residues in the second peptide (222–237, Fig. 8, purple) completely buried. Residues 205–221 correspond to a short region where the predicted secondary structures of NDV-F and RSV-F disagree (Fig. 6B), suggesting a possible local difference in structure. Nevertheless the sections of protein that bury these residues, 60–80 in F_2 and 468–480 in F_1, are in areas of high confidence in the model. This observation implies that antibodies specific to these regions interact when the residues are exposed in some different conformation of RSV-F, such as the pre-fusogenic form of the protein or an intermediate that appears during the conversion from the pre- fusogenic to the fusogenic form.

Conclusion

We have described a novel assay for RSV-F function that allows quantitative measurement of the effect of RSV-F inhibitors on the induction of cellular fusion and allows rapid testing of the effect of specific mutations on protein function without the complication of mutagenesis of the viral genome. Because this assay correlates well with experimental data for the inhibition of viral function *in vitro*, we have used it to characterize a series of drug escape mutants isolated using serial passage in the presence of inhibitors. Three recently described RSV-F-specific fusion inhibitors were used to select resistant viruses and the point mutations associated with resistance identified.

We have also shown that the homology model of RSV-F presented here is supported by experimental evidence including gross morphology derived from EM images and the position and nature of antibody binding sites. The sites associated with inhibitor resistance were mapped on to the validated model, allowing the compounds to be grouped into two classes. Correlation between the location of the mutations and the model structure has provided hypotheses for the mechanisms by which the two classes of fusion inhibitors function. We propose that one class functions by disrupting the formation of the helical core region of the protein through binding within or near the hydrophobic binding pocket in the trimeric core occupied by F488. We hypothesize that a second class of fusion inhibitor, represented by compound 3, interacts with a region of basic residues within the RSV-F head and perturbs F function, perhaps through interference of F interaction with a cellular GAG target. A number of neutralizing antibodies that bind to a site overlapping this region may well act in a similar manner. It is anticipated that these observations will allow the continued rational development of new inhibitors of RSV-F action.

Materials and methods

Cells and virus

HEp-2 cells (American Type Culture Collection (ATCC), Rockville, MD, USA) were maintained in Eagle's minimal essential medium (Biowhittaker, Walkerville, MD, USA) containing 10% gamma-irradiated fetal bovine serum (FBS) (Invitrogen New Zealand Ltd, Auckland, New Zealand) and 1% L-glutamine (Biowhittaker Walkerville, MD, USA). RSV A2 (VR-1302) strain, RSV Long (VR-26) strain, and RSV B-1 (VR-1400) strain were purchased from ATCC and grown in HEp-2 cells. 293 cells were also purchased from ATCC.

Recombinant RSV-F constructs, mutagenesis, and expression studies

Single-stranded synthetic DNA oligonucleotides encoding portions of RSV A2 F glycoprotein incorporating optimal codons (Haas et al., 1996) and without potential poly(A) addition or splice sites were generated synthetically. These oligonucleotides, of average length 60 bases, were annealed and ligated together to produce three fragments: (1) a 631-bp *Pst*I–*Mfe*I fragment, (2) a 606-bp *Mfe*I–*Xho*I fragment, and (3) a 379-bp *Xho*I–*Bam*HI fragment. The gel-purified fragments were cloned into the pLitmus vector. The full-length gene was assembled by sequential cloning into the CMV expression vector pCICO, a derivative of pJW4304 (kindly provided by J. Mullins, Department of Microbiology, University of Washington (Chapman et al., 1991)), which contains a full-length CMV promoter, CMV authentic intron sequence, SV40 early region 3′ terminator, and SV40 origin of replication. The construct encoding the soluble form of the recombinant glycoprotein lacking sequences encoding the transmembrane and cytoplasmic tail domains was titled pCICO.Fopt. A membrane-anchored full-length F was generated by insertion of a 270-bp *Eco*RI–*Xbu*I fragment encoding the transmembrane and cytoplasmic domains of RSV-F into pCICO.Fopt to yield pCICO.F.FL.opt.

The RSV-F synthetic sequence was designed to include unique restriction sites approximately every 50 to 100 bases.

This enabled the use of cassette mutagenesis to rapidly mutate any region of the molecule. In brief, oligonucleotides containing the desired mutation were assembled in double-stranded fragments and cloned into the appropriate restriction sites of the RSV-F synthetic gene. Mutations were routinely confirmed by sequencing the replaced region.

Expression levels of F were assayed by transient $CaPO_4$ precipitation-mediated transfection assays in 293 cells. Cells in a 60-mm dish were transfected with 5 μg of plasmid and 0.5 μg of pVARNA (Groskreutz and Schenborn, 1994). Expressed proteins were radiolabeled by incubation for 5 h in the presence of [^{35}S]methionine and cysteine 24 h posttransfection. Cell lysates and supernatants were immunoprecipitated with an RSV-F-specific monoclonal antibody and the precipitates were analyzed by polyacrylamide gel electrophoresis. Gels were impregnated with scintillant, dried, and exposed to X-ray film.

Synthetic constructs for codon-optimized RSV-G and RSV-SH were produced in a similar manner and used for coexpression studies with the RSV-F construct. Expression levels of both proteins were assessed by radiolabeling and immunoprecipitation as for RSV-F above.

Syncytium formation assay

Fusion activity of the RSV-F constructs was measured in 293 cells. Cells in six-well plates (Corning) at approximately 50% confluency were transfected by adding plasmid DNA (2 μg/well) carrying the constructs of interest in $CaPO_4$ solution for 4 h followed by a 15% glycerol shock and then washed with PBS. To each well, 2 ml growth medium was added and the cells were incubated at 37°C in a 5% CO_2 incubator and observed 24–48 h posttransfection. The F-transfected cells are identical in appearance to RSV-F-infected cells, being characterized by the presence of many large syncytia and dying cells due to the fusion of cellular membranes by the expressed F protein. Control cells were confluent at the same time point.

For quantitative assay, transfected cells, after glycerol shock and wash, were trypsinized and transferred to 96-well plates containing dilutions of inhibitor. Cells from one well of a six-well plate were distributed to 30 wells of a 96-well plate. Syncytium formation was quantified at 48 h posttransfection by addition of 20 μl of CellTiter 96 One solution (Promega) and incubation for 1 to 4 h at 37°C. The color reaction was then stopped by addition of 25 μl 10% SDS to each well and the difference in absorbance of the well at 492 and 690 nm measured. EC_{50} values were determined from the absorbance data by computer curve fitting. Fusion inhibitors were assayed by exposing transfected cells to half-log serial dilutions of inhibitors with the reduction in scorable syncytium formation used as a direct measurement of the efficacy of the inhibitor. Results from the F-specific syncytium formation assay and RSV viral CPE assays were comparable in both relative potency of inhibitors tested and the susceptibility of F variants bearing resistance mutations (Figs. 2 and 4, Table 1).

RSV CPE reduction assay

All test compounds were synthesized by Biota. Serial threefold dilutions of test compounds were prepared in 96-well tissue culture plates containing 100 μl per well of assay medium (Eagle's minimal essential medium (MEM) supplemented with 2% fetal bovine serum and glutamine alanyl-L-glutamine). Human laryngeal carcinoma (HEp-2) cells were trypsinized and diluted in assay medium to a concentration of 1.5×10^5 viable cells/ml. One hundred microliters of the diluted cells was added to each of several individual wells of each 96-well plate and designated as uninfected control wells. The remaining cell suspension was infected with RSV at a multiplicity of infection of 0.2 – 0.05 PFU per cell depending on virus strain used. The cell–virus suspension was mixed well by inversion and 100 μl was immediately dispensed into the remaining wells of the 96-well plates. Assay plates were incubated in a 37°C incubator for 5 days. Viral replication was quantified by determination of cell viability substantially as described by Watanabe and colleagues (1994). Briefly, 100 μl of 3 mg/ml MTT (3-(4,5-dimethylthiazol-2-yl)-2,5-diphenyltetrazolium bromide) was added to each well and plates were incubated at 37°C in a 5% CO_2 incubator for 2 h. Wells were aspirated to dryness and the crystalline product of MTT metabolism was dissolved by addition of 200 μl of 100% isopropanol. The extent of metabolism was measured via determination of absorbance using a computer-controlled microplate reader at 540 nm with a reference wavelength of 690 nm (Denizot and Lang, 1986). The 50% effective concentration (EC_{50}) was determined using computer curve fitting.

Viral plaque assay and selection of drug-resistant virus

HEp-2 cells were seeded at a density of 8×10^5 cells/well and grown until fully confluent in six-well plates (Corning, Acton, MA, USA). Cells were infected with approximately 2×10^5 PFU of RSV in the presence of 0.1, 1 or 10 μg/ml of compound 1 or 2. After adsorption for 1 h at 37°C the virus inoculum was replaced by an agarose (Sigma Chemical Co., St Louis, MO, USA) overlay supplemented with 2% FBS, 1% L-glutamine, and the same concentration of compound 1 or 2. Plaques were allowed to develop for 3 days. Plaques were picked and expanded in the presence of compound 1 or 2 in HEp-2 cells at the same concentration as used initially. Resistant virus to compound 3 was generated by limit dilution passaging over six passages, with the drug concentration ranging from an initial 0.25 μg/ml to a final concentration of 2 μg/ml. Putative resistant virus (evident by the presence of viral cytopathology in these cultures) was recovered. RNA isolated, and the F gene sequence determined via RT-PCR. Viruses were considered resistant to an inhibitor if the EC_{50} value was shifted by at least 10-fold compared with the co-passaged parental virus. To test for drug resistance/cross-resistance, larger-scale virus stocks were grown, titered, F gene resequenced, and assayed for drug resistance using the assay described above.

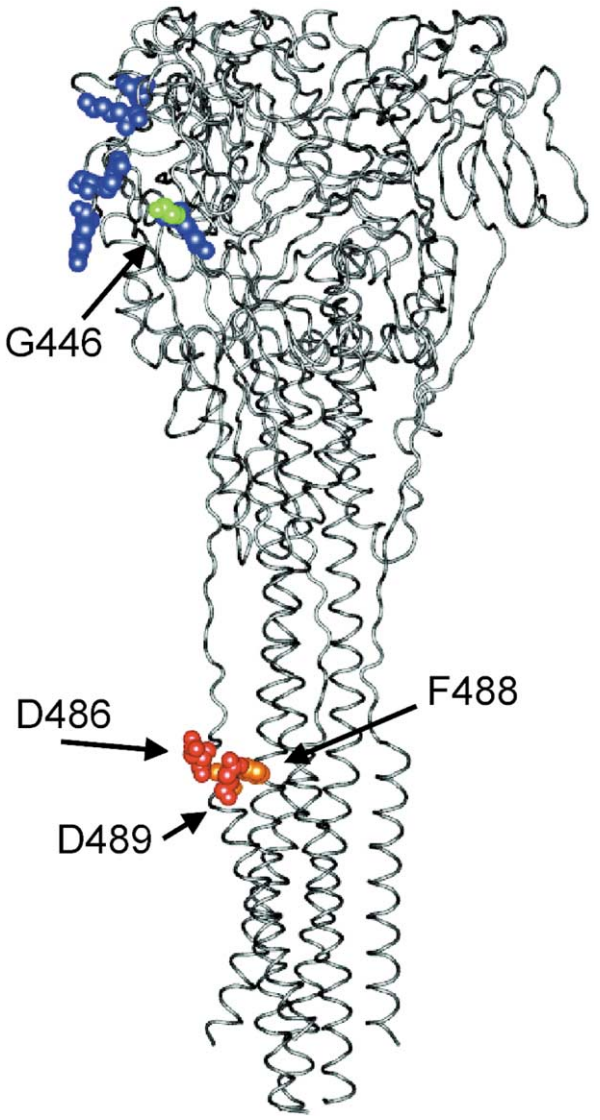

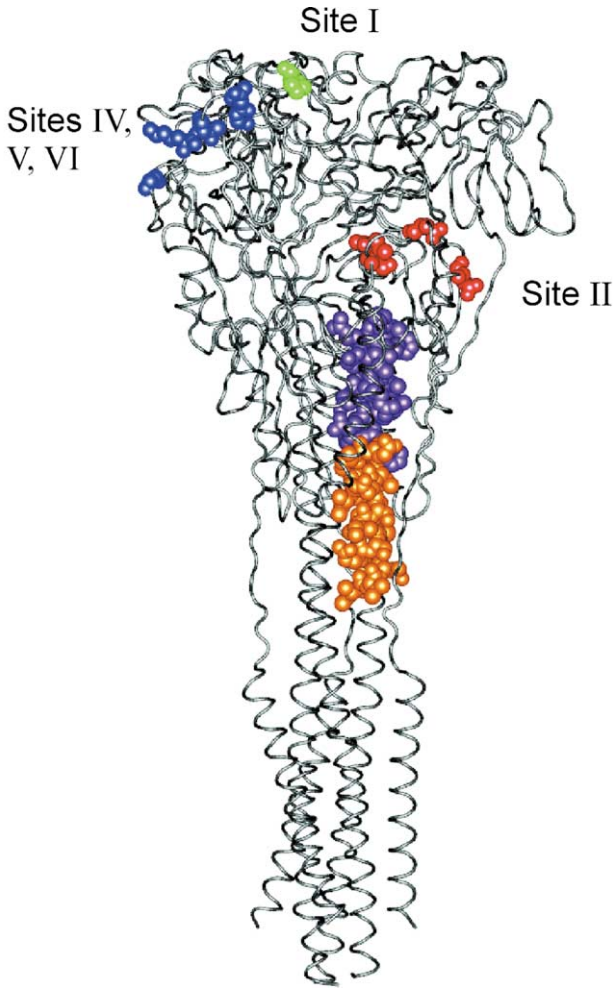

Fig. 7. Structure of RSV-F showing the position of several escape mutants that allow continued RSV-F activity in the presence of three specific fusion inhibitors: (1) VP14637 (Patent WO 99/38508), (2) R170591 (Patent WO 01/00612), and (3) CL-387626 (Wyde et al., 1998). The residues where escape mutations for compounds 1 and 2 are found are shown as spheres (D486, D489 red; F488 yellow) on one of the three F2 chains and cluster in the HR-A helix over a hydrophobic pocket in the surface of the internal HR-B helices of the core domain. For compound 3, resistance mutation arises at a second site on the head of the RSV-F molecule The central glycine residue (G446, shown in green) gives rise to resistance on mutation to a glutamate. The cluster of basic residues around the glycine believed to interact with the inhibitor is highlighted (blue).

Fig. 8. Location of several antigenic sites on the RSV-F model structure. The majority of the protein is shown as a gray backbone trace, with residues contributing to antigenic sites shown as color-coded spheres. Site I is shown in green, Site II in red, and Sites IV, V, and VI, which overlap, in blue. The correlation between Sites IV, V, and VI and the location of the resistance mutation for compound 3 (Fig. 7) is clear. Two contiguous peptides give rise to RSV-neutralizing antibodies in animals; residues 205–221 (orange) and 222–237 (purple) are indicated. These residues are almost completely buried in the RSV-F model, suggesting that they are available for antibody binding in a different conformation of the protein.

In the case of multiple mutations arising in a putative resistant virus, the importance of each substitution was determined by separate assay in the syncytium formation assay (Mason et al., 2000) described above (see Table 1).

Model building

As a preliminary step in modeling the RSV-F protein a chimeric construct of the NDV-F structure and the RSV-F core structure was produced. This chimera was built using SwissPDB Viewer (SPDBV, Guex and Peitsch, 1997) by superimposing the coordinates of G184-Q202 of chain A from the RSV-F core onto G171-Q189 of chain A in the NDV-F structure. These residues were selected after conducting alignment of the amino acid sequence of the two proteins from which it was determined that they were structurally equivalent regions. The superimposition revealed an excellent correspondence in structure, allowing completion

of the chimera by manual editing of the combined PDB files. The chimeric structure was subject to energy minimization of the four-residue stretches either side of the six joining points to remove any minor errors that the manual combination of structures had introduced. The chimera was then used as the basis for building a model of RSV-F. Note that the sequence used for RSV-F corresponds to the RSV strain A2 clone in use in the Biota Virology Laboratory and differs in five sites from GenBank Entry AAB59858.1 (E66K, P101Q, P102A, I379V, and M447V). A single loop (residues A412 to S425 in RSV-F) was not able to be built in a satisfactory manner using an automated alignment (CLUSTAL (Thompson et al., 1994)) of the RSV-F and chimera sequences and was manually adjusted on the basis of PHD secondary structure prediction (Rost et al., 1994) and the maintenance of a conserved disulfide bond, with the final alignment shown in Fig. 6B. The two chains of each F_1–F_2 pair were initially modeled as separate entities in SPDBV, with manual inspection of the candidate loops for each mismatch used to select the optimal structure. A total of 10 loop structures were rebuilt (1 in F_2 and 9 in F_1).

The separate RSV-F1 and RSV-F2 structures were then combined and the complete trimeric RSV-F structure was assembled by superimposing on each of the subunits of the chimera. Minimization of the complete RSV-F model was carried out with Discover in the InsightII package (Accelrys Inc., CA, USA) under the cvff forcefield to remove undesirable interactions that had been generated by the modeling process. First, the residues surrounding each inserted loop were minimized with the rest of the structure held fixed to correct any minor mismatches at insertion points. Then the backbone atoms of the whole protein were held fixed and the side chain atoms minimized using Steepest Descent minimization until the maximum gradient value dropped to below 10. The backbone constraints were then removed and the whole structure was allowed to minimize for a further 100 steps of Steepest Descent minimization. Superposition of the final model with the coordinates of the NDV-F fragment and RSV core structures gave backbone RMSDs for common residues of 1.03 and 1.37 Å, respectively. The completed model of RSV-F was assessed using the Verify3D program (Eisenberg et al., 1997) which showed that the model was of acceptable quality. More than 93% of residues in the model had backbone geometry in the favorable region of a Ramachandran plot.

Large-scale expression and purification of recombinant RSV-F

The RSV (A2 strain) F gene was amplified by RT-PCR with oligonucleotide primers designed to incorporate *Bam*HI restriction sites for subsequent cloning into the baculovirus shuttle vector, pAcYM1.his. This vector was derived from pAcYM1 by insertion of an oligonucleotide fragment encoding a histidine tag into the *Bam*HI site. Subsequent expression of cloned inserts produced recombinant proteins with a fused C-terminal His tag. The F gene was amplified to include the N-terminal signal sequence but was truncated at the C terminus to remove the transmembrane and cytoplasmic domains. This vector was cotransfected along with linearized BacPac6 baculoviral DNA into *Spodoptera frugiperda* cells. Recombinant baculoviruses were selected on the basis of F protein secretion into the culture medium and virus stocks were subsequently prepared. High-titered recombinant virus stocks were used to infect Hi5 cells in suspension culture and medium harvests were collected at 48 h postinfection. Harvests were clarified by centrifugation followed by filtration through 22-nm filters before concentration and buffer exchange by tangential flow ultrafiltration. The concentrated preparations were passed through a Ni^{2+}-affinity column (Ni-NTA Agarose, Qiagen, Germany), the column was washed, and bound protein was eluted with 100 mM imidazole. Elution fractions containing recombinant F protein were assessed by SDS–PAGE analysis, pooled, and then concentrated by filtration (Centricon-50). SDS–PAGE analysis revealed that all preparations comprised a doublet (see Fig. 5A), reflecting incomplete cleavage at the F_2/F_1 junction as well as at a second proteolytic activation site originally identified by us (Mason et al., 2000) and recently also described by others (Gonzalez-Reyes et al., 2001; Zimmer et al., 2001), at the N terminus of the RSV-F unique sequence.

Electron microscopy

Recombinant F protein was diluted in phosphate-buffered saline to approximately 10 μg/ml. Droplets of approximately 5 μl of this solution were applied to thin carbon films on 400-mesh copper grids which had been glow-discharged in nitrogen for 30 s. After 1 min the excess protein solution was drawn off, followed by washing in approximately 5 μl PBS, then 2–3 droplets of 2% uranyl formate (prepared as described in Russell and Hyder, 1976) was added for 1 min. The grids were air-dried and then examined at 80 kV in a JEOL 100B transmission electron microscope at a magnification of 100,000x. Electron micrographs were recorded on Kodak SO-163 film and developed in undiluted Kodak D19 developer. The electron-optical magnification was calibrated by comparison with the width of tobacco mosaic virus (180Å) imaged under similar conditions (calibration virus was a gift from Adrian Gibbs, Australian National University).

Acknowledgments

We thank Keith Watson, Roland Nearn, Tomislav Karoli, and Julia Ciani for synthesis of the inhibitors and Anjali Sahasrabudhe for sequencing the compound 3 resistance mutants. We also thank Mike Lawrence and David Chalmers for helpful discussions.

References

Bourgeois, C., Corvaisier, C., Bour, J.B., Kohli, E., Pothier, P., 1991. Use of synthetic peptides to locate neutralizing antigenic domains on the fusion protein of respiratory syncytial virus. J. Gen. Virol. 72, 1051–1058.

Calder, L.J., Gonzalez-Reyes, L., Gracia-Barreno, B., Wharton, S.A., Skehel, J.J., Wiley, D.C., Melero, J.A., 2000. Electron microscopy of the human respiratory syncytial virus fusion protein and complexes that it forms with monclonal antibodies. Virology 271, 122–131.

Cane, P.A., 2001. Molecular epidemiology of respiratory syncytial virus. Rev. Med. Virol. 11, 103–116.

Chambers, P., Pringle, C.R., Easton, A.J., 1990. Heptad repeat sequences are located adjacent to hydrophobic regions in several types of virus fusion glycoproteins. J. Gen. Virol. 71, 3075–3080.

Chambers, P., Pringle, C.R., Easton, A.J., 1992. Sequence analysis of the gene encoding the fusion glycoprotein of pneumonia virus of mice suggests possible conserved secondary structure elements in paramyxovirus fusion glycoproteins. J. Gen. Virol. 73, 1717–1724.

Chapman, B.S., Thayer, R.M., Vincent, K.A., Haigwood, N.L., 1991. Effect of intron A from human cytomegalovirus (Towne) immediate-early gene on heterologous expression in mammalian cells. Nucleic Acids Res. 19, 3979–3980.

Chen, L., Gorman, J.J., McKimm-Breschkin, J., Lawrence, L.J., Tulloch, P.A., Smith, B.J., Colman, P.M., Lawrence, M.C., 2001. The structure of the fusion glycoprotein of Newcastle disease virus suggests a novel paradigm for the molecular mechanism of membrane fusion. Structure 9, 255–266.

Collins, P.L., McIntosh, K., Chanock, R.M., 1996. Respiratory syncytial virus, in: Fields, B.N., Knipe, D.M., Howely, P.M. (Eds.), Field's Virology, 3rd ed. Lippincott–Raven, Philadelphia.

Denizot, F., Lang, R., 1986. Rapid colorimetric assay for cell growth and survival: modifications to the tetrazolium dye procedure giving improved sensitivity and reliability. J. Immunol. Methods 89, 271–277.

Eckert, D.M., Malashkevich, V.N., Hong, L.H., Carr, P.A., Kim, P.S., 1999. Inhibiting HIV-1 entry: discovery of D-peptide inhibitors that target the gp41 coiled-coil pocket. Cell 99, 103–115.

Eisenberg, D., Luthy, R., Bowie, J.U., 1997. VERIFY3D: assessment of protein models with three-dimensional profiles. Methods Enzymol. 277, 396–404.

Gonzalez-Reyes, L., Begona Ruiz-Arguello, M., Garcia-Barreno, B., Cladér, L., Lopez, J.A., Albar, J.P., Skehel, J.J., Wiley, D.C., Melero, J.A., 2001. Cleavage of the human respiratory syncytial virus fusion protein at two distinct sites is required for activation of membrane fusion. Proc. Natl. Acad. Sci. USA 98, 9859–9864.

Groskreutz, D., Schenborn, E., 1994. Increased gene expression in mammalian cells lines using pAdVAntage DNA as a co-transfectant. Promega Notes Magazine 48, 8.

Guex, N., Peitsch, M.C., 1997. SWISS-MODEL and the Swiss-Pdb Viewe: an environment for comparative protein modeling. Electrophoresis 18, 2714–2723.

Haas, J., Park, E.C., Seed, B., 1996. Codon usage limitation in the expression of HIV-1 envelope glycoprotein. Curr. Biol. 6, 15–324.

Hallak, L.K., Spillman, D., Collins, P.L., Peeples, M.E., 2000. Glycosaminoglycan sulfation requirements for respiratory syncytial virus infection. J. Virol. 74, 10508–10513.

Heminway, B.R., Yu, Y., Tanaka, Y., Perrine, K.G., Gustafson, E., Bernstein, J.M., Galinski, S., 1994. Analysis of respiratory syncytial virus F, G and SH protein in cell fusion. Virology 200, 801–805.

Kahn, J.S., Schnell, M.J., Buonocore, L., Rose, J.K., 1999. Recombinant vesicular stomatitis virus expressing respiratory syncytial virus (RSV) glycoproteins: RSV fusion protein can mediate infection and cell fusion. Virology 254, 81–91.

Karger, A., Schmidt, U., Buchholz, U.J., 2000. Recombinant bovine respiratory syncytial virus with deletions of the G and SH genes: G and F proteins bind heparin. J. Gen. Virol. 82, 631–640.

Lawless-Delmedico, M.K., Sista, P., Sen, R., Moore, N.C., Antczak, J.B., White, J.M., Greene, R.J., Leanza, K.C., Matthews, T.J., Lambert, D.M., 2000. Heptad-repeat regions of respiratory syncytial virus F1 protein form a six-membered coiled-coil complex. Biochemistry 39, 11684–11695.

Lopez, J.A., Andreu, D., Carreno, C., Whyte, P., Taylor, G., Melero, J.A., 1996. Conformational constraints of conserved neutralising epitopes from a major antigenic area of human respiratory syncyital virus fusion protein. J. Gen. Virol. 77, 649–660.

Lopez, J.A., Bustos, R., Orvell, C., Berois, M., Arbiza, J., Garcia-Barreno, B., Melero, J.A., 1998. Antigenic structure of human respiratory syncytial virus fusion glycoprotein. J. Virol. 72, 6922–6928.

Martinez, I., Melero, J.A., 2000. Binding of human respiratory syncytial virus to cells: implication of sulfated cell surface proteoglycans. J. Gen. Virol. 81, 2715–2722.

Mason, A., Young, P.R., Tucker, S.P., November 2000. Method of expression and agents identified thereby. U.S. Patent 60/262,767.

Matthews, J.M., Young, T.F., Tucker, S.P., Mackay, J.P., 2000. The core of the respiratory syncytial virus fusion protein is a trimeric coiled coil. J. Virol. 74, 5911–5920.

Monto, A.S., Lim, S.K., 1971. The Tecumseh study of respiratory illness. 3. Incidence and periodicity of respiratory syncytial virus and *Mycoplasma pneumoniae* infections. Am. J. Epidemiol. 94, 290–301.

Rost, B., Sander, C., Schneider, R., 1994. PHD—an automatic mail server for protein secondary structure prediction. Comput. Appl. Biosci. 10, 53–60.

Russell, E.R., Hyder, M.L., 1976. The thermal decomposition of uranyl formate and the preparation of ammonium uranyl formate, $(NH_4)UO_2(COOH)_4$. Inorg. Nucl. Chem. Lett. 12, 247–250.

Smith, B.J., Lawrence, M.C., Colman, P.M., 2002. Modelling the structure of the fusion protein from human respiratory syncytial virus. Protein Eng. 15, 365–371.

Techaarpornkul, S., Barretto, N., Peeples, M.E., 2001. Functional analysis of recombinant respiratory syncytial virus deletion mutants lacking the small hydrophobic and/or attachment glycoprotein. J. Virol. 75, 6825–6834.

Thompson, J.D., Higgins, D.G., Gibson, T.J., 1994. CLUSTAL W: improving the sensitivity of progressive multiple sequence alignment through sequence weighting, position-specific gap penalties and weight matrix choice. Nucleic Acids Res. 22, 4673–4680.

Toiron, C., Lopez, J.A., Rivas, G., Andreu, D., Melero, J.A., Bruix, M., 1996. Conformational studies of a short linear peptide corresponding to a major conserved neutralizing epitope of human respiratory syncytial virus fusion glycoprotein. Biopolymers 39, 537–548.

Trudel, M., Nadon, F., Seguin, C., Dionne, G., Lacroix, M., 1987. Identification of a synthetic peptide as a part of a major neutralization epitope of respiratory syncytial virus. J. Gen. Virol. 68, 2273–2280.

Watanabe, W., Konno, K., Ijichi, K., Inoue, H., Yokota, T., Shigeta, S., 1994. MTT colorimetric assay system for the screening of anti-orthomyxo- and anti-paramyxoviral agents. J. Virol. Methods 48, 257–265.

Wyde, P.R., Moore-Poveda, D.K., O'Hara, B., Ding, W.-D., Mitsner, B., Gilbert, B.E., 1998. CL387626 exhibits marked and unusual antiviral activity against respiratory syncytial virus in tissue culture and in cotton rats. Antiviral Res. 38, 31–42.

Zhao, X., Singh, M., Malashkevich, V.N., Kim, P.S., 2000. Structural characterization of the human respiratory syncytial virus fusion protein core. Proc. Natl. Acad. Sci. USA 97, 14172–14177.

Zhou, G., Ferrer, M., Chopra, R., Kapoor, T.M., Strassmaier, T., Weissenhorn, W., Skehel, J.J., Oprian, D., Schreiber, S.L., Harrison, S.C., Wiley, D.C., 2000. The structure of an HIV-1 specific cell entry inhibitor in complex with the HIV-1 gp41 trimeric core. Bioorg. Med. Chem. 8, 2219–2227.

Zimmer, G., Budz, L., Herrler, G., 2001. Proteolytic activation of respiratory syncytial virus fusion protein: cleavage at two furin consensus sequences. J. Biol. Chem. 276, 31642–31650.